Edge states in rationally terminated honeycomb structures

Charles L Fefferman, Sonia Fliss, Michael I Weinstein

EDGE STATES IN RATIONALLY TERMINATED HONEYCOMB STRUCTURES

C.L. FEFFERMAN[(1)], S. FLISS[(2)], AND M. I. WEINSTEIN[(3)]

Abstract. Consider the tight binding model of graphene, sharply terminated along an edge $\mathbf{l}$ parallel to a direction of translational symmetry of the underlying period lattice. We classify such edges $\mathbf{l}$ into those of "zigzag type" and those of "armchair type", generalizing the classical zigzag and armchair edges. We prove that zero energy/flat band edge states arise for edges of zigzag type, but never for those of armchair type. We exhibit explicit formulae for flat band edge states when they exist. We produce strong evidence for the existence of dispersive (non flat) edge state curves of nonzero energy for most $\mathbf{l}$.

keywords: Graphene | edge state |tight binding | spectrum

A phenomenon of great interest in Materials Science is the propagation of electrons along line-defects or *edges* in a crystalline material. It was first recognized by [5, 8] that edge transport depends on the shape of the edge. We study the spectrum arising from the tight-binding model of graphene, sharply terminated along a rational edge, i.e. an edge $\mathbf{l}$ parallel to a direction of translational symmetry of the underlying period lattice. Unlike standard "zigzag" and "armchair" edges, a general rational edge gives rise to edge states with nonzero energies and non-flat dispersion curves. We report numerical evidence for such states, as well as a rigorous analysis that determines precisely when zero-energy ("flat band") edge states arise. We set up basic definitions and notation and then state our results. Detailed proofs of our rigorous results, and explanations of our numerical investigations, are presented in [4].

1. The Honeycomb Structure, $\mathbb{H}$

The Honeycomb Structure, $\mathbb{H}$, consists of all the vertices of all the tiles in a tiling of the plane by regular hexagons. $\mathbb{H}$ is invariant under translations by vectors in the *equilateral triangular lattice* $\Lambda = \mathbb{Z}\mathring{\mathbf{v}}_1 \oplus \mathbb{Z}\mathring{\mathbf{v}}_2$, where we may take $\mathring{\mathbf{v}}_1 = (\sqrt{3}/2, 1/2)$ and $\mathring{\mathbf{v}}_2 = (\sqrt{3}/2, -1/2)$. More precisely, we may express $\mathbb{H}$ as the union of two interpenetrating triangular lattices: $\mathbb{H} = \left(\mathring{\mathbf{v}}_A + \Lambda\right) \cup \left(\mathring{\mathbf{v}}_B + \Lambda\right) \equiv \mathbb{H}_A \cup \mathbb{H}_B$, where $\mathring{\mathbf{v}}_A = 0$ and $\mathring{\mathbf{v}}_B = \frac{1}{3}\left(\mathring{\mathbf{v}}_1 + \mathring{\mathbf{v}}_2\right)$. The points of $\mathbb{H}_A$ and $\mathbb{H}_B$ are called, respectively, "$A-$sites" and "$B-$sites". Each site $\omega \in \mathbb{H}$ has three nearest neighbors in $\mathbb{H}$; we denote the set of those three nearest neighbors $\mathrm{NN}(\omega)$.

2. The Terminated Honeycomb Structure, $\mathbb{H}_\sharp$

Any straight line $\mathbf{l}$ separates the plane into two half-planes $\Omega^{\pm}$. We pick one of these halfspaces, Ω^+, and the *terminated structure,* $\mathbb{H}_\sharp$ *arising from* $\mathbf{l}$ is defined as $\mathbb{H} \cap \Omega^+$. We restrict our attention to *rational edges*, *i.e.* we assume that the line $\mathbf{l}$ is parallel to a nonzero

Date: This manuscript was compiled on December 4, 2022.

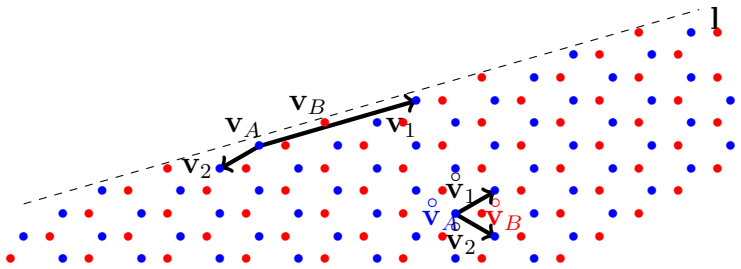

FIGURE 1. Notation for the honeycomb structure.

vector in the lattice Λ. Other classes of terminated structures were considered by [1,3]; see the section below on the relation of the current work to previous works. Given a rational edge, we may pick an alternative triangular lattice basis for Λ, one of whose elements is parallel to $\mathbf{l}$; see Figure 1. To do so, first, choose relatively prime integers a_{11} and a_{12} such that the vector

$$\mathbf{v}_1 = a_{11}\mathring{\mathbf{v}}_1 + a_{12}\mathring{\mathbf{v}}_2 \tag{2.1}$$

is parallel to $\mathbf{l}$. Further, we may choose integers a_{21} and a_{22} such that $\det(a_{ij}) = 1$, and the vector

$$\mathbf{v}_2 = a_{21}\mathring{\mathbf{v}}_1 + a_{22}\mathring{\mathbf{v}}_2 \tag{2.2}$$

points into Ω^+. The integers a_{21} and a_{22} are not uniquely determined but our results are independent of the choice of these integers.

To describe $\mathbb{H}_\sharp$ in terms of the basis $\{\mathbf{v}_1, \mathbf{v}_2\}$ we introduce the integers: $s_1, s_2 \in \{-1, 0, 1\}$ as follows:

$$a_{22} - a_{21} \equiv s_1, \text{ modulo } 3 \tag{2.3a}$$

$$a_{11} - a_{12} \equiv s_2, \text{ modulo } 3. \tag{2.3b}$$

The plane can be tiled by parallelograms whose sides are translates of $\mathbf{v}_1$ and $\mathbf{v}_2$. Each such parallelogram contains exactly one $A-$site and one $B-$site. For one such parallelogram, those sites are, respectively,

$$\mathbf{v}_A = 0, \quad \mathbf{v}_B = \frac{1}{3}(s_1\mathbf{v}_1 + s_2\mathbf{v}_2). \tag{2.3c}$$

For integers $n^A_{\min}$, $n^B_{\min}$, our terminated honeycomb $\mathbb{H}_\sharp$ is then given by

$$\begin{aligned}\mathbb{H}_\sharp = &\{\mathbf{v}_A + m\mathbf{v}_1 + n\mathbf{v}_2 \big| (m,n) \in \mathbb{Z}^2,\ n \geq n^A_{\min}\} \\ &\cup \{\mathbf{v}_B + m\mathbf{v}_1 + n\mathbf{v}_2 \big| (m,n) \in \mathbb{Z}^2,\ n \geq n^B_{\min}\}\end{aligned} \tag{2.4}$$

Our results depend only on $n^A_{\min} - n^B_{\min}$ because they are independent of the shift of $n^A_{\min}$ and $n^B_{\min}$ together by an arbitrary integer; this amounts to an integer translate of $\mathbb{H}_\sharp$ in the direction $\mathbf{v}_2$. One can show that $n^A_{\min} - n^B_{\min} \in \{0, s_2\}$. If $n^A_{\min} = n^B_{\min}$, we say that $\mathbb{H}_\sharp$ is a *balanced* terminated honeycomb (in this case for each parallelogram, mentioned before, which overlaps with $\mathbb{H}_\sharp$, its $A-$site and $B-$site lie inside $\mathbb{H}_\sharp$) ; otherwise we say that $\mathbb{H}_\sharp$ is an *unbalanced* terminated honeycomb (in this case there are parallelograms whose $A-$site lies

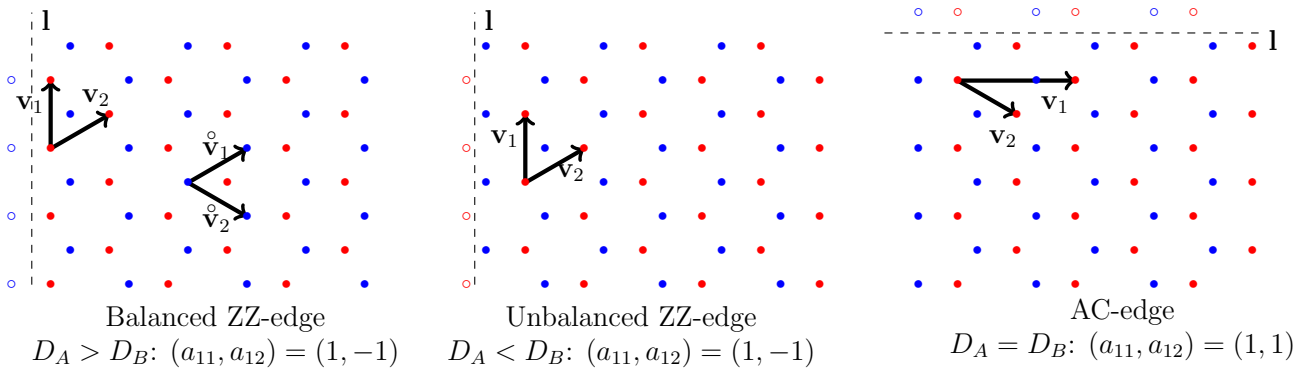

FIGURE 2. $\mathbb{H}_\sharp$ for the classical ZZ and AC edges, balanced and unbalanced. $A-$ sites are in blue and $B-$ sites are in red. The edge, $\mathbf{l}$, is indicated with a dashed line.

in $\mathbb{H}_\sharp$ but whose $B-$site does not lie in $\mathbb{H}_\sharp$; or else whose $B-$site lies in $\mathbb{H}_\sharp$ but whose $A-$site does not lie in $\mathbb{H}_\sharp$).

3. Zigzag-type and Armchair-type Edges

We present geometric and arithmetic characterizations of the types of edges that arise via our honeycomb termination procedure.

First, by translation invariance with respect to the vector $\mathbf{v}_1$, there is a row of $A-$sites in $\mathbb{H}_\sharp$ with minimal distance $D_A \geq 0$ to the line $\mathbf{l}$ and similarly a row of $B-$sites in $\mathbb{H}_\sharp$ with minimal distance $D_B \geq 0$ to the line $\mathbf{l}$.

We say that $\mathbb{H}_\sharp$, the terminated structure arising from $\mathbf{l}$, or simply its edge, is of *Zigzag-type (ZZ)* if $D_A \neq D_B$ and we say that it is of *Armchair-type (AC)* if $D_A = D_B$. It can be proven that ZZ-type edges are those for which the integers defined in (2.1), satisfy $a_{11} - a_{12} = \pm 1 \bmod 3$ (i.e. $s_2 = \pm 1$) and AC-type edges are such that $a_{11} - a_{12} = 0 \bmod 3$ (i.e. $s_2 = 0$). Note that ZZ-type edges could be balanced or unbalanced whereas the AC-type edges could only be balanced.

The best known edges correspond to the choices: (1) $\mathbf{v}_1 = \mathring{\mathbf{v}}_1$ (or equivalently $\mathbf{v}_1 = \mathring{\mathbf{v}}_1 - \mathring{\mathbf{v}}_2$), the classical zigzag edges: (balanced/ordinary or unbalanced/bearded); and (2) $\mathbf{v}_1 = \mathring{\mathbf{v}}_1 + \mathring{\mathbf{v}}_2$, the classical armchair edge; see Figure 2.

4. The Tight-binding Hamiltonian, $H_\sharp$ associated with $\mathbb{H}_\sharp$

Our Hamiltonian acts on "wave functions" $\psi = (\psi_\omega)_{\omega \in \mathbb{H}_\sharp}$ with each $\psi_\omega \in \mathbb{C}$; ψ_ω is the quantum amplitude of ψ at site ω. We define the Hamiltonian $H_\sharp$ by the formula

$$(H_\sharp \psi)_\omega = \sum_{\omega' \in \mathrm{NN}(\omega) \cap \mathbb{H}_\sharp} \psi_{\omega'} \tag{4.1}$$

We may Fourier analyze $H_\sharp$ by virtue of the invariance of $\mathbb{H}_\sharp$ under translation by the vector $\mathbf{v}_1$. Given $k \in [0, 2\pi)$, a *k-pseudoperiodic wave function* is a vector $\psi = (\psi_\omega)_{\omega \in \mathbb{H}_\sharp}$ such that $\psi_{\omega + \mathbf{v}_1} = e^{ik} \psi_\omega$ for all $\omega \in \mathbb{H}_\sharp$. There is a natural l^2 norm on k-pseudoperiodic wave functions, given by summing $|\psi_\omega|^2$ over equivalence classes modulo translations by multiples of $\mathbf{v}_1$. We write $l^2_k(\mathbb{H}_\sharp)$ to denote the space of k-pseudoperiodic wave functions with finite l^2 norm. The

Hamiltonian $H_\sharp$ maps $l^2_k(\mathbb{H}_\sharp)$ to itself as a bounded self-adjoint operator. We write $H_{\sharp,k}$ to denote the restriction of $H_\sharp$ to $l^2_k(\mathbb{H}_\sharp)$.

We are interested in the spectral theory of the operator $H_\sharp$ acting in the space $l^2(\mathbb{H}_\sharp)$. By translation invariance with respect to $\mathbf{v}_1$ this can be reduced to the spectral theory of $H_{\sharp,k}$ for $k \in [0, 2\pi)$. In particular, we want to understand eigenvectors of $H_{\sharp,k}$, which are called *edge states*, *i.e.* pairs (E, ψ) such that $H_{\sharp,k}\psi = E\psi$ and $0 \neq \psi \in l^2_k(\mathbb{H}_\sharp)$. By definition, an edge state is plane-wave like under translation by $\mathbf{v}_1$ (parallel to the edge), but the amplitudes ψ_ω decay to zero as the distance from ω to the edge tends to infinity. If $E = 0$ is an edge state eigenvalue for k ranging over a subinterval of $[0, 2\pi)$ then we refer to the corresponding family of edge states as a *zero energy / flat band of edge states* of $H_\sharp$.

We next state one of the main results of this article.

Theorem 1: Complete classification of zero energy / flat band edge states of $H_\sharp$ for rational edges. Assume $k \in [0, 2\pi]$.

- For any armchair edge ($D_A = D_B$), there are no zero-energy edge states.
- All zigzag edges ($D_A \neq D_B$) give rise to a flat band of zero-energy edge states for k varying in a proper quasi-momentum subset of $[0, 2\pi]$. These states are supported either exclusively on the $A-$ sites of $\mathbb{H}_\sharp$ ($A-$site ES) or exclusively on the $B-$sites of $\mathbb{H}_\sharp$ ($B-$site ES). Whenever $H_{\sharp,k}$ has a zero energy edge state, the space of such states is one-dimensional.

A complete classification is given in the table below:

	$D_A < D_B$	$D_B < D_A$
Balanced	A-site ES for $k \in I$	B-site ES for $k \in I$
Unbalanced	A-site ES for $k \in [0, 2\pi] \setminus \overline{I}$	B-site ES for $k \in [0, 2\pi] \setminus \overline{I}$

TABLE 1. Description of all zero energy edge states. ($I = (\frac{2\pi}{3}, \frac{4\pi}{3})$)

5. Representation formulae for zero energy / flat band edge states

Each edge state is expressible as a linear combination of exponential solutions of the bulk difference equations, which (a) decay into the bulk and (b) satisfies the boundary conditions that ψ_ω vanishes at all vertices of $\mathbb{H}$ which are outside $\mathbb{H}_\sharp$. These decaying exponential solutions are associated with the roots of an appropriate polynomial, which depends on the edge parameters (a_{ij}): $p_+(\zeta; k)$ for $B-$ site edge states and $p_-(\zeta; k)$ for $A-$ site edge states. In particular, $p_+(\zeta; k)$ and $p_-(\zeta; k)$ are polynomials of degree $n_3 - n_1$, where n_ν ($\nu = 1, 2, 3$) are introduced in the detailed mathematical setup below.

In Theorem 1, edge states occur only if we are in the zigzag case; $a_{11} - a_{12} \neq 0 \mod 3$. Let $r = r(k)$ denote the number of zeros of the relevant polynomial inside the open unit disc and denote these roots by:

$$\zeta_j = \zeta_j(k), \quad 1 \leq j \leq r(k). \tag{5.1}$$

For $k \notin \{2\pi/3, 4\pi/3\}$, we have proved in [4] that

$$r(k) = \begin{cases} -n_1 - s_2 \mathbb{1}_{(2\pi/3, 4\pi/3)}(k), & \text{for } p_+ \\ n_3 + s_2 \mathbb{1}_{(2\pi/3, 4\pi/3)}(k), & \text{for } p_- \end{cases} \tag{5.2}$$

where $\mathbb{1}_S(k)$ denotes the indicator function of the set S. The cases $k = 2\pi/3, 4\pi/3$ are dealt with separately in [4].

Furthermore assume that k lies in an appropriate subinterval of $[0, 2\pi]$ for which there are edge states; see the above table in Theorem 1. In the following result, we let $n^A_{\min}$, $n^B_{\min}$ be as in (2.4) and n_ν, for $\nu = 1, 2, 3$, be as defined in the detailed mathematical setup below.

Theorem 2 [Representation formulae] Denote the nonzero components of a zero energy edge state ψ by

$$\psi_{\mathbf{v}_I + m\mathbf{v}_1 + n\mathbf{v}_2} = e^{imk}\Psi(n;k) \quad \text{for } m \in \mathbb{Z},\ n \geq n^I_{\min}$$

where $I = A$ or B, according to whether the edge state is supported on A-sites or B-sites. Let n_{base} defined by:

$$n_{\text{base}} = \begin{cases} n^B_{\min} - n_3, & \text{if} \quad I = A \\ n^A_{\min} + n_1, & \text{if} \quad I = B \end{cases} \tag{5.3}$$

Then,

$$\Psi(n;k) = c\tilde{\Psi}(n),$$

where c is an arbitrary complex constant and $\tilde{\Psi}(n)$ is given by the three equivalent formulas for $n \geq n_{\text{base}}$:

$$\tilde{\Psi}(n) = \sum_{\substack{\ell_1+\cdots+\ell_r = n - n_{\text{base}}+1 \\ \ell_1,\ldots,\ell_r \geq 1}} \zeta_1^{\ell_1 - 1} \cdots \zeta_r^{\ell_r - 1}, \tag{5.4}$$

$$\tilde{\Psi}(n) \ = \ \frac{1}{2\pi}\int_0^{2\pi} e^{i(n-n_{\text{base}}+1)\omega} \prod_{j=1}^{r} \left(e^{i\omega} - \zeta_j\right)^{-1} d\omega, \tag{5.5}$$

$$\tilde{\Psi}(n) = \sum_{j=1}^{r} \frac{\zeta_j^{n-n_{\text{base}}}}{\prod_{\ell \in \{1,\ldots,r\}\setminus\{j\}} (\zeta_\ell - \zeta_j)}. \tag{5.6}$$

For $n < n_{\text{base}}$, $\tilde{\Psi}(n) = 0$.
For the normalization, we have

$$\|\tilde{\Psi}\|^2_{l^2(\mathbb{Z})} = \sum_{j=1}^{r} \frac{\zeta_j^{r-1}}{1 - |\zeta_j|^2} \prod_{\ell \in \{1,\ldots,r\}\setminus\{j\}} \frac{1}{(\zeta_\ell - \zeta_j)(1 - \overline{\zeta_j}\zeta_\ell)}\ . \tag{5.7}$$

Note that this representation formula reduces to the standard formula for the zero energy edge states in the case of the classical zigzag edges (for which $r = 1$ and $\zeta_1 = (1 + e^{\imath k})^{\pm 1}$).

6. Non-zero energy (dispersive) edge states

We have designed and implemented a numerical method to compute edge states and their associated dispersion curves. All computations were performed in MATLAB using the computer code available in `https://osf.io/6z874/`. A brief review of numerical investigations, with focus on $E \neq 0$ edge states, appears below; see also [4]. For $\mathbb{H}_\sharp$ terminated by a rational edge other than the standard zigzag and armchair, we find non-zero energy, non-flat band (hence dispersive) edge states as shown in Figure 3; in each figure the intersection of the dark region with the vertical line corresponding to a fixed k is the spectrum of $H_{\sharp,k}$. In particular, the curved lines bifurcating out of the (Dirac) points: $(E, k) = (0, 2\pi/3)$ and

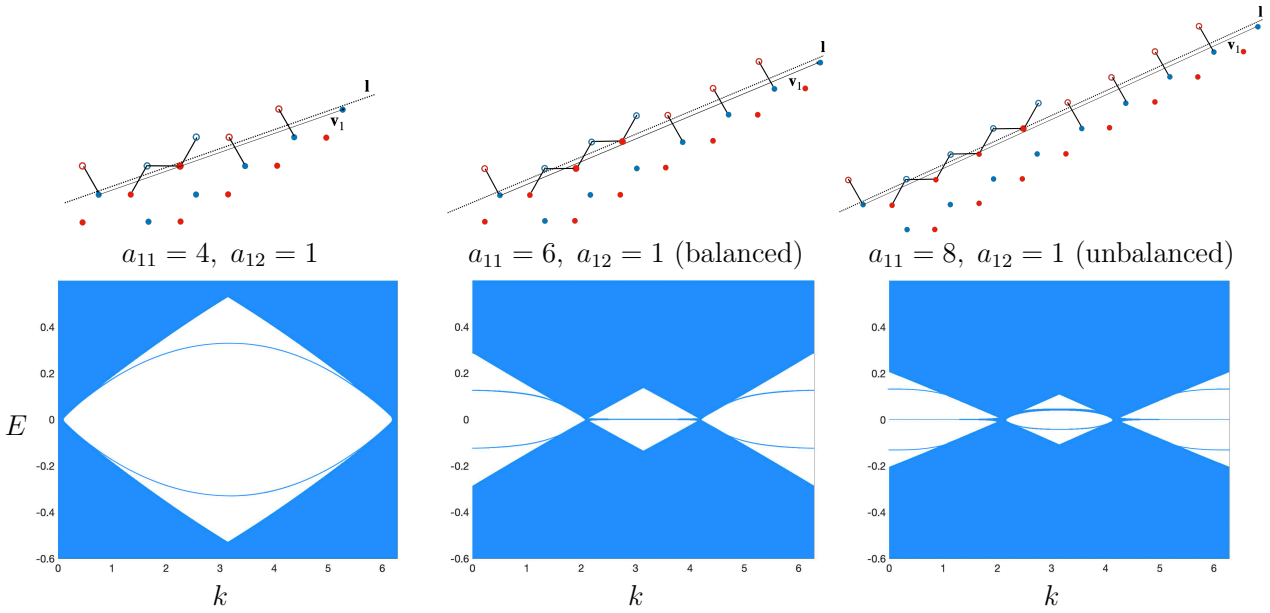

FIGURE 3. l_k^2 spectrum of $H_{\sharp,k}$ versus k for several choices of edges: (i) $(a_{11}, a_{12}) = (4, 1)$, an AC-type edge, (ii) $(a_{11}, a_{12}) = (6, 1)$, a ZZ-type balanced edge and (iii) $(a_{11}, a_{12}) = (8, 1)$, a ZZ-type unbalanced edge. Above each plot, a diagram of the associated edge with the bonds that connect the sites in the structure closest to the boundary (also called frontier sites and represented with filled circles) to the closest sites outside the structure (represented with empty circles).

$(0, 4\pi/3)$ (middle and right figures), and $(E, k) = (0, 0)$ and $(E, k) = (0, 2\pi)$ (left figure), parametrize non-flat band edge states.

7. Relation to previous works

The tight binding edge Hamiltonian has most commonly been studied for the classical zigzag and armchair edges; see Figure 2. In [6] it is proved that the classical armchair edge supports no edge modes (zero or nonzero energy). Our rigorous analytical results on edge states for general rational edges appear to be new.

There are studies in the physics literature of rational edges [1,2,7]. The definitions of edges used in these works differ from ours. Let us now describe these classes of edges, and contrast them with the class of edges studied in this article. Recall that our edges are boundaries of structures $\mathbb{H}_\sharp \subset \mathbb{H}$, comprised of all honeycomb vertices in a closed half-space determined by a line parallel to $\mathbf{v}_1$, where $\mathbf{v}_1$ is any vector in the triangular lattice Λ. Here, we shall refer to such edges as *half-space termination edges*.

The notion of *minimal edge* was introduced in [1]. Minimal edges have the following properties:

- the structure is periodic with period vector $\mathbf{v}_1 = a_{11}\mathring{\mathbf{v}}_1 + a_{12}\mathring{\mathbf{v}}_2$, where $a_{11}, a_{12}$are positive integers,

- no site of $\mathbb{H}_\sharp$ has two nearest neighbors in $\mathbb{H} \setminus \mathbb{H}_\sharp$,
- no site of $\mathbb{H} \setminus \mathbb{H}_\sharp$ has two nearest neighbors in $\mathbb{H}_\sharp$,
- within a period, there are precisely $a_{11} + a_{12}$ frontier sites, i.e. sites of $\mathbb{H}_\sharp$ with neighbors in $\mathbb{H} \setminus \mathbb{H}_\sharp$.

See Figure 4 (left) for an example of a minimal edge. It is suggested in [1] that such minimal edge structures are energetically preferred. In general, a minimal edge need not be of the half-space termination type studied here.

The class of *modified edges*, arising from the periodic attachment of atoms and bonds to minimal edge atoms at frontier sites of $\mathbb{H}_\sharp$, is studied in [7]. The edges studied here may be either minimal or modified (see Figure 4) .

In [2], edges which arise from a periodic pattern of displacements of a selected dimer (pair of nearest neighbor sites) are studied, with period vector $\mathbf{v}_1 = a_{11}\mathring{\mathbf{v}}_1 + a_{12}\mathring{\mathbf{v}}_2$ with $a_{11}, a_{12} \in \mathbb{Z}$. In the case where $a_{11}, a_{12} > 0$, this class of edges is asserted to be precisely the class of minimal edges, as defined in [1]. There is overlap between our class of half-space termination edges and those discussed in [2], but neither class includes the other.

We now compare our results with those of [1, 2, 7]. The main goal of [1] is to derive continuum boundary conditions for an effective Dirac operator, associated with a minimal rational edge. Toward this goal, they consider the tight binding model for parallel quasimomentum $k \approx 0$. The article [2] postulates a *bulk-edge correspondence*: for a fixed edge, the dimension of the subspace of zero energy edge states is equal to the winding number of the Zak phase along a one-dimensional Brillouin zone determined by the edge orientation. The authors of [2] apply this approach to obtain an expression, derived previously in [1], for the density of edge states. The reader should note that the results of [2] are displayed in terms of a scaled (edge-dependent) parallel quasi-momentum range, while the range of parallel quasimomenta in the present article is fixed to be $[0, 2\pi]$. There appears to be agreement between our rigorous results and the results in [2] for those edges in the overlap of our studies. To our knowledge, no previous articles rigorously address, for a general class of rational edges, the questions of: which parallel quasimomentum ranges support zero energy edge states; when they exist, the dimensionality of the eigenspaces; whether the edge states are supported on $A-$ or $B-$ sublattice sites; or explicit formulae for zero energy edge states.

Numerical studies in [7] indicate that a flat band, for a minimal edge, can give rise to non-zero energy edge state curves when additional sites and bonds are attached to form a modified edge. Our numerical investigations give strong evidence that non-zero energy edge state curves arise in minimal structures themselves.

8. Detailed mathematical setup and ideas behind our results

We first give an explicit formulation of the edge state eigenvalue problem for the Hamiltonian $\mathbb{H}_\sharp$ defined in (4.1). By (2.3b) there are integers k_1 and k_2 such that $a_{11} - a_{12} = 3k_2 + s_2$ and $a_{22} - a_{21} = 3k_1 + s_1$, where $s_1, s_2 \in \{-1, 0, 1\}$. Now set $\tilde{m}_1 = k_1$, $\tilde{n}_1 = k_2$, $\tilde{m}_2 = k_1 + a_{21}$, $\tilde{n}_2 = k_2 - a_{11}$, $\tilde{m}_3 = k_1 - a_{22}$ and $\tilde{n}_3 = k_2 + a_{12}$. Except for the classical zigzag case ($\mathbf{v}_1 = \mathring{\mathbf{v}}_1$), which we analyze separately, the integers $\tilde{n}_1, \tilde{n}_2$ and $\tilde{n}_3$ are all distinct. We define $m_\nu = \tilde{m}_{\sigma(\nu)},\ n_\nu = \tilde{n}_{\sigma(\nu)}),\ \nu = 1, 2, 3$, where σ is the permutation of $\{1, 2, 3\}$, such that

$$\tilde{n}_{\sigma(1)} < \tilde{n}_{\sigma(2)} < \tilde{n}_{\sigma(3)}.$$

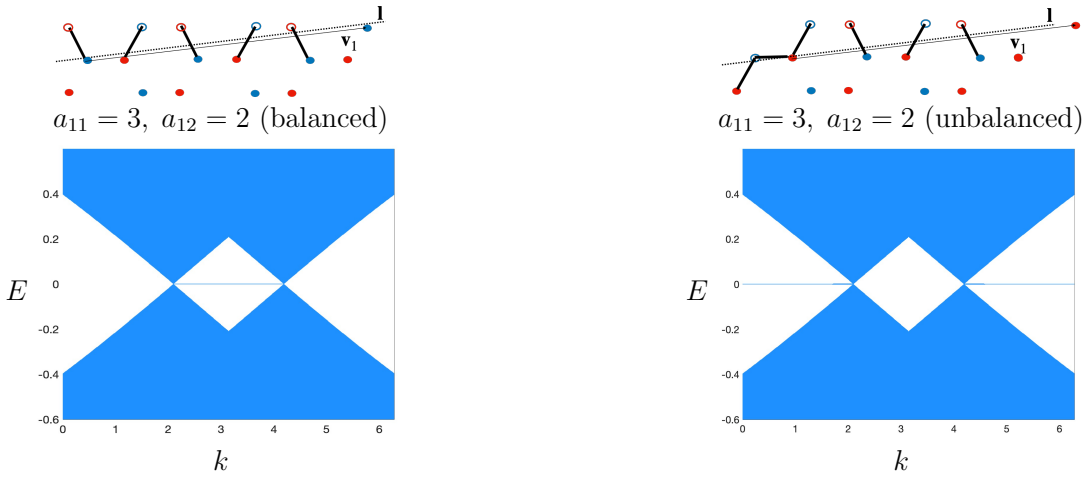

FIGURE 4. l^2_k spectrum of $H_{\sharp,k}$ versus k for the ZZ-type edge $(a_{11}, a_{12}) = (3, 2)$, : (left) balanced and (right) unbalanced. Note that the balanced edge is minimal whereas the unbalanced one is not.

The three nearest neighbors in $\mathbb{H}$ to the A-site $\mathbf{v}_A + m\mathbf{v}_1 + n\mathbf{v}_2$ are the three $B-$sites:

$$\mathbf{v}_B + (m + m_\nu)\mathbf{v}_1 + (n + n_\nu)\mathbf{v}_2, \quad \nu = 1, 2, 3,$$

and the three nearest neighbors in $\mathbb{H}$ to the B-site $\mathbf{v}_B + m\mathbf{v}_1 + n\mathbf{v}_2$ are the three $A-$sites:

$$\mathbf{v}_A + (m - m_\nu)\mathbf{v}_1 + (n - n_\nu)\mathbf{v}_2, \quad \nu = 1, 2, 3.$$

A wave function in l^2_k may be written in the form

$$\psi(\mathbf{v}_A + m\mathbf{v}_1 + n\mathbf{v}_2) = e^{imk}\psi^A(n), \quad n \geq n^A_{\min} \tag{8.1a}$$

$$\psi(\mathbf{v}_B + m\mathbf{v}_1 + n\mathbf{v}_2) = e^{imk}\psi^B(n), \quad n \geq n^B_{\min} \tag{8.1b}$$

where $m \in \mathbb{Z}$.

9. The edge state eigenvalue problem

The wave function in (8.1) is an edge state for energy E if and only if ψ^A,ψ^B satisfy the difference equations and boundary conditions:

$$\sum_{\nu=1,2,3} e^{im_\nu k}\psi^B(n + n_\nu) = E\psi^A(n), \quad n \geq n^A_{\min} \tag{9.1a}$$

$$\psi^B(n) = 0, \quad n < n^B_{\min}, \tag{9.1b}$$

and

$$\sum_{\nu=1,2,3} e^{-im_\nu k}\psi^A(n - n_\nu) = E\psi^B(n), \quad n \geq n^B_{\min} \tag{9.2a}$$

$$\psi^A(n) = 0, \quad n < n^A_{\min}. \tag{9.2b}$$

10. On the proof of Theorem 1 on zero energy / flat band edge states

When $E = 0$, (9.1) and (9.2) decouple. We shall discuss (9.1) here, the equation governing edge states which are supported on $B-$ sites; (9.2), governing edge states which are supported on $A-$sites, is addressed analogously.

Solutions of (9.1) are related to roots, $\zeta = \zeta(k)$, located within the open unit disc, of the *indicial equation*

$$\sum_{\nu=1,2,3} e^{im_\nu k}\zeta^{n_\nu} = 0. \tag{10.1}$$

or equivalently of the $n_3 - n_1$ degree polynomial equation: $p_+(\zeta, k) \equiv 1 + e^{i(m_2-m_1)k}\zeta^{n_2-n_1} + e^{i(m_3-m_1)k}\zeta^{n_3-n_1} = 0$.

As in (5.1) we denote these roots by $\zeta_j = \zeta_j(k)$, $j = 1, \dots, r(k)$, where we recall that $r = r(k)$ is the number of roots of the polynomial equation (10.1) inside the open unit disc. Since all the roots can be proven to be simple, any solution of (9.1) is given by

$$\psi^B(n) = \sum_{j=1}^{r} A_j\zeta_j^n, \quad \text{for} \quad n \geq n^A_{\min} + n_1, \tag{10.2a}$$

$$\psi^B(n) = 0, \quad n < n^A_{\min} + n_1, \tag{10.2b}$$

where $(A_1, \dots, A_r)$ is an arbitrary solution of the linear algebraic system

$$\sum_{j=1}^{r} \zeta_j^n A_j = 0, \quad n^A_{\min} + n_1 \leq n < n^B_{\min} \tag{10.3}$$

Note that $n^A_{\min} + n_1 \leq n^B_{\min}$. Indeed, we have already observed that $n^B_{\min} - n^A_{\min} \in \{0, -s_2\}$, and we prove in Appendix A.4 of [4] that $n_1 \leq -1$. Thus, non-trivial $B-$site edge states exist for those $k \in [0, 2\pi]$ for which (10.3) has a non-trivial solution $(A_1, \dots, A_r)$. Since the number of independent equations in (10.3) is $n^B_{\min} - n^A_{\min} - n_1$ and there are $r(k)$ unknowns, a nontrivial $B-$site edge state for energy $E = 0$ exists if and only if

$$r(k) > n^B_{\min} - n^A_{\min} - n_1. \tag{10.4}$$

Furthermore, if (10.4) holds, then the dimension of the zero energy eigenspace is equal to $r(k) - [n^B_{\min} - n^A_{\min} - n_1]$. The expression for $r(k)$ is displayed in (5.2). To deduce Theorem 1 from (10.4), we use the expression for $r(k)$ and the following formula, proved in [4], for $D_B - D_A$ in terms of $s_2, n^B_{\min}$ and $n^A_{\min}$:

$$D_B - D_A = \frac{\sqrt{3}}{2}|\mathbf{v}_1|^{-1}\left(\frac{1}{3}s_2 + n^B_{\min} - n^A_{\min}\right).$$

An analogous argument yields the result for $A-$site edge states.

11. On the proof of Theorem 2 on representation formulae for zero energy / flat band edges states

Here, we explain our derivation of our explicit formulae for zero energy edge states. (5.4) can be reduced to the following result. Let $\zeta_1, \dots, \zeta_r$ denote distinct complex numbers. Then,

there exist $A_1, \dots, A_r \in \mathbb{C}$ such that

$$\text{For all } \ n \geq 1, \quad \sum_{\substack{k_1+\cdots+k_r=n \\ k_1,\dots,k_r\geq 1}} \zeta_1^{k_1} \cdots \zeta_r^{k_r} = \sum_{j=1}^{r} A_j \zeta_j^n. \tag{11.1}$$

Note, in particular, that this expression vanishes for $1 \leq n < r$. (11.1) is proven by induction on the number r. (5.5) follows from (5.4) by a discrete Fourier Transform and finally (5.6) is obtained from (5.5) by residue calculation.

12. Remarks on the numerical investigation of $E \neq 0$ edge states

When $E \neq 0$, equations (9.1)-(9.2) are no longer uncoupled. As in the $E = 0$ case, solutions are represented as a linear combination of exponential solutions, $\zeta^n \xi$, where $\xi = (\xi^A, \xi^B) \in \mathbb{C}^2 \setminus \{0\}$ and $\zeta \in \mathbb{C}$ such that the following equations hold.

$$P_+(\zeta, k) \cdot P_-(\zeta, k) = E^2, \quad \text{where} \tag{12.1a}$$

$$P_+(\zeta, k) = \sum_{\nu=1,2,3} e^{i m_\nu k} \zeta^{n_\nu}, \quad P_-(\zeta, k) = \sum_{\nu=1,2,3} e^{-i m_\nu k} \zeta^{-n_\nu}, \tag{12.1b}$$

with m_ν, n_ν as defined earlier; and when ζ solves (12.1), there exists a nonzero vector $(\xi^A, \xi^B) \in \mathbb{C}^2$ that satisfies

$$\begin{pmatrix} -E & P_+(\zeta, k) \\ P_-(\zeta, k) & -E \end{pmatrix} \begin{pmatrix} \xi^A \\ \xi^B \end{pmatrix} = \begin{pmatrix} 0 \\ 0 \end{pmatrix}. \tag{12.2}$$

If E is not in the essential spectrum [9] of $H_\sharp(k)$, we can prove that (12.1) has $n_3 - n_1$ roots inside the open unit disc (and no roots on the unit circle); we denote them by $\zeta_1, \dots, \zeta_{n_3-n_1}$ (not to be confused with the roots listed in (5.1)) and denote the corresponding ξ as (ξ_j^A, ξ_j^B). The ζ_j, ξ_j^A, ξ_j^B depend on E and k. The vector (ξ_j^A, ξ_j^B) is defined up to a multiplication by a nonzero complex scalar. We assume that the ζ_j are all distinct. The vector (ξ_j^A, ξ_j^B) can then be taken to depend analytically on E as E varies in a small complex disk.

The analogue of (10.3), governing edge states whose energies, E, are not constrained to be zero, is the $(n_3 - n_1) \times (n_3 - n_1)$ system of homogeneous linear equations

$$\sum_{j=1}^{n_3-n_1} \zeta_j^n \xi_j^A \cdot A_j = 0, \quad \text{for} \quad n_{\min}^B - n_3 \leq n < n_{\min}^A \tag{12.3a}$$

$$\sum_{j=1}^{n_3-n_1} \zeta_j^n \xi_j^B \cdot A_j = 0, \quad \text{for} \quad n_{\min}^A + n_1 \leq n < n_{\min}^B \tag{12.3b}$$

for unknowns $A_1, \dots, A_{n_3-n_1}$. An edge state with quasimomentum $k \in [0, 2\pi]$ and energy E occurs if and only if the determinant of the coefficient matrix of the linear system (12.3), $\Delta(E, k)$, is equal to zero.

We have numerically investigated the edge state eigenvalue problem, for different choices of rational edge termination, by studying the function $(E, k) \mapsto \Delta(E, k)$ over a discrete grid with respect to E and k of different resolutions. The discrete values of k vary in the interval $I_k = [0, 2\pi]$ in Figures 3 and 4 and in the interval $I_k = [0, \pi]$ in Figures 5 and 6; those of E vary between rigorous bounds on the spectrum of $H_\sharp$. More precisely, given (k, E), we may carry out the following algorithm:

- Compute the $2(n_3 - n_1)$ roots of (12.1). The roots are calculated by computing the eigenvalues of the associated companion matrix. We verify the assumption that the roots, ζ, are distinct.
- Deduce whether E is in the essential spectrum of $H_\sharp(k)$(if one of the roots lies on the unit circle) or not.
- Compute, for each root $\zeta(k, E)$ inside the unit circle, a vector satisfying (12.2).
- Construct the matrix $\mathbb{M}(k, E)$ appearing in (12.3) and compute its determinant $\Delta(k, E)$.

We make a *heat map* of the function $(k, E) \mapsto \log|\Delta(k, E)|$ over the regular $(N_k+1)\times(N_E+1)$ grid of points of $I_k \times (-E_{\rm lim}, E_{\rm lim})$ where $N_k, N_E = 1000$. In Figure 3, the dark areas correspond to the essential spectrum. Outside the dark areas, we seek edge state curves by studying where $(k, E) \mapsto \log|\Delta(k, E)|$ takes on very large negative values. The function $E \mapsto |\Delta(k, E)|$ appears to vanish at $E = 0$ for $k \in (2\pi/3, 4\pi/3)$, for the ZZ-type edges (middle and right figures) but not to vanish at $E = 0$ for all $k \in (0, 2\pi)$ for the AC-type edge (left figure). This illustrates Theorem 1.

To confirm existence of an edge state near a particular point $(k, E) = (k_0, E_0)$, we compute the winding number of the mapping $E \mapsto \Delta(k_0, E)$ along a sufficiently small circle about E_0, which makes sense because the mapping is analytic. In all the investigated cases, the winding number is equal to one, implying that there exists a simple root of $E \mapsto \Delta(k_0, E)$ near E_0.

Finally, we study the behavior of the spectrum as the length of the period vector increases. We consider first a sequence of armchair type edges defined by $a_{12} = 1$ as a_{11} increases. We observe the presence of multiple dispersive (non-flat) edge state curves bifurcating from $(k, E) = (0, 0)$ (and from $(k, E) = (2\pi, 0)$), we find that the number of curves increases when a_{11} increases. Figure 5 showing the cases $a_{11} = 10$ and $a_{11} = 22$ illustrates the increasing complexity of the dispersion curves. Similar observations hold for balanced zigzag-like edges; see Figure 6. Note that as a_{11} tends to infinity, the sequence of edges studied (a_{11} increasing and $a_{12} = 1$) tends to the balanced classical zigzag edge. Although the classical zigzag edge has a single dispersion curve, which is flat only over a limited range of k, the nearly flat dispersion curves in Figures 5 and 6 extend over all $k \in (0, 2\pi)$. Note however that the definition of quasimomentum depends on the edge. On the other hand, we have studied a sequence of edges for which a_{11} and a_{12} are two consecutive Fibonacci numbers and we find no evidence for such increasing complexity.

13. Summary and open questions

We have completely analyzed the question of which rational edges give rise to zero energy / flat band edge states. We have given formulae for these edge states when they exist. Finally, we have given a general criterion for the existence of edge states (dispersive or non-dispersive) that we have implemented numerically.

Many natural open questions arise from this study (for an extended list, see [4]) and we mention two of them. Note that our results do not determine all rational edges that give rise ONLY to zero-energy edge states. Indeed, while the classical armchair edge has no edge states (flat band or dispersive), we have shown that, more generally, an edge of "armchair-type" produces no zero energy edge states but it can produce dispersive edge state curves of

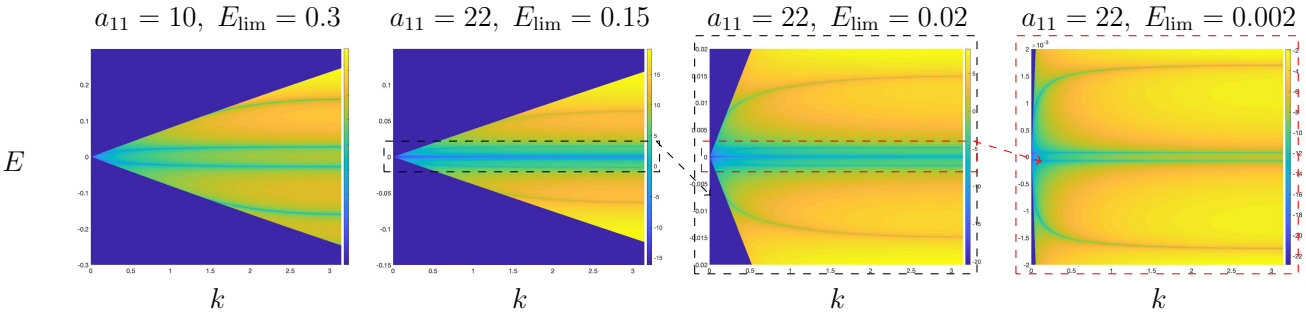

FIGURE 5. Plots of $(k, E) \mapsto \log|\Delta(E, k)|$ for $k \in (0, \pi)$ ($N_k = 1000$ points) and $E \in (-E_{\rm lim}, E_{\rm lim})$ ($N_E = 1000$ points) for various armchair-like edges with $a_{12} = 1$.

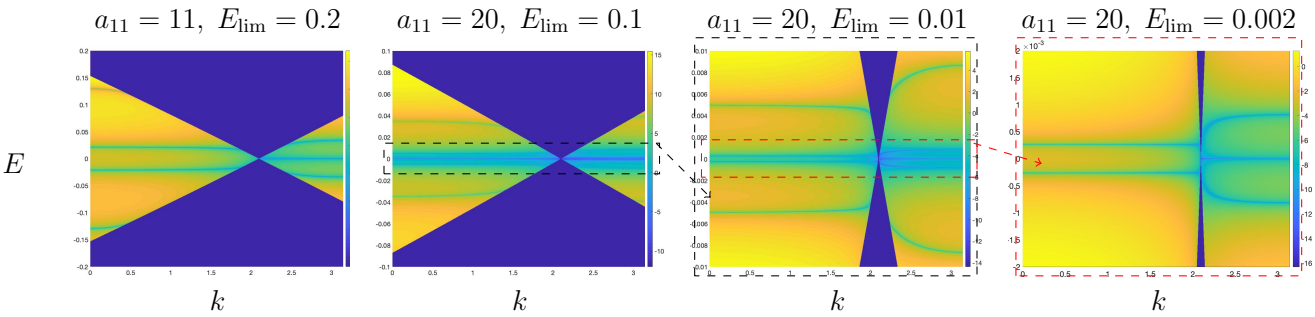

FIGURE 6. Plots of $(k, E) \mapsto \log|\Delta(E, k)|$ for $k \in (0, \pi)$ ($N_k = 600$ points) and $E \in (-E_{\rm lim}, E_{\rm lim})$ ($N_E = 600$ points) for various ordinary zigzag-like edges with $a_{12} = 1$.

non-zero energy. A mathematically rigorous understanding of precisely which edges give rise to dispersive edge states, in particular an understanding of the bifurcation of the dispersive curves in terms of the values (a_{11}, a_{12}), would be of interest. Finally, the main motivation of the present study was to understand transport along irrational edge terminations and we hope to use the results presented here as a first step.

14. Aknowledgments

This research was initiated at a working group on "Irrational edges" at the American Institute of Mathematics (AIM) Workshop on the *Mathematics of Topological Insulators*, December 7-11, 2020, which was supported by the American Institute of Mathematics, the US National Science Foundation, the Simons Foundation and Columbia University. C.L.F. was supported in part by National Science Foundation grant DMS-1700180. M.I.W. was supported in part by National Science Foundation grants DMS-1620418 and DMS-1908657 as well as Simons Foundation Math + X Investigator Award #376319. We warmly thank the participants of the AIM working group, as well as Pierre Delplace, David Gontier and Mikael Rechtsman for stimulating discussions.

References

[1] AR Akhmerov and CWJ Beenakker, *Boundary conditions for Dirac fermions on a terminated honeycomb lattice*, Physical Review B **77** (2008), no. 8, 085423.

[2] P Delplace, D Ullmo, and G Montambaux, *Zak phase and the existence of edge states in graphene*, Physical Review B **84** (2011), no. 19, 195452.

[3] Pierre Delplace, D Ullmo, and G Montambaux, *Zak phase and the existence of edge states in graphene*, Physical Review B **84** (2011), no. 19, 195452.

[4] C.L. Fefferman, S. Fliss, and M.I. Weinstein, *Discrete honeycombs, rational edges and edge states*, https:.

[5] M. Fujita, K. Wakabayashi, K. Nakada, and K. Kusakabe, *Peculiar localized state at zigzag graphite edge*, J. Phys. Soc. Jpn. **65** (1996), 1920–1923.

[6] G. M. Graf and M. Porta, *Bulk-edge correspondence for two-dimensional topological insulators*, Comm. Math. Phys. **324** (2012), no. 3, 851–895.

[7] W. Jaskolski, A. Ayuela, M. Pelc, H. Santos, and L. Chico, *Edge states and flat bands in graphene nanoribbons with arbitrary geometries edge states and flat bands in graphene nanoribbons with arbitrary geometries*, Phys. Rev. B **83** (2011), 235424.

[8] Kyoko Nakada, Mitsutaka Fujita, Gene Dresselhaus, and Mildred S Dresselhaus, *Edge state in graphene ribbons: Nanometer size effect and edge shape dependence*, Physical Review B **54** (1996), no. 24, 17954.

[9] M. Reed and B. Simon, *Methods of modern mathematical physics: Analysis of operators, volume iv*, Academic Press, 1978.

(1) Department of Mathematics, Princeton University, Princeton, NJ, USA
Email address: cf@math.princeton.edu

(2) POEMS (CNRS-Inria-ENSTA Paris), Institut Polytechnique de Paris, Palaiseau, France
Email address: sonia.fliss@ensta-paris.fr

(3) Department of Applied Physics and Applied Mathematics and Department of Mathematics, Columbia University, New York, NY, USA
Email address: miw2103@columbia.edu